ELSEVIER

Catalysis Today 50 (1999) 399–412

CATALYSIS TODAY

Effect of ceria on palladium supported catalysts for high temperature combustion of CH_4 under lean conditions

G. Groppi*, C. Cristiani, L. Lietti, C. Ramella, M. Valentini, P. Forzatti

Politecnico di Milano, Dipartimento di Chimica Industriale ed Ingegneria Chimica "G. Natta", Piazza Leonardo da Vinci 32, 20133, Milan, Italy

Abstract

The effects of CeO_2 and La_2O_3 addition to alumina-supported palladium catalysts have been investigated. Characterization of the promoted and unpromoted supports has been performed by XRD, TPR, L-Raman and surface area measurements. Supported Pd catalysts have been characterized by means of XRD and TG analyses.

TG analyses on palladium catalysts confirm the occurrence of reversible $PdO \Leftrightarrow Pd^0$ transformation in the presence of O_2 and show that such palladium redox process is markedly affected by CeO_2. In presence of ceria, temperatures of reduction of PdO and reoxidation of Pd^0 are both shifted 50–60°C above the corresponding temperature observed on unpromoted samples.

Activity tests in CH_4 combustion under lean conditions show that the addition of ceria on La_2O_3-stabilized alumina does not significantly affect light-off performances, but markedly affects the catalytic combustion behavior at high temperature in line with ceria effect of stabilization of active PdO species.

Keywords: Methane combustion; Pd-supported catalysts; PdO species; PdO decomposition/separation

1. Introduction

In the last decades catalytic combustors for natural gas fueled gas turbines (GT) have attracted increasing attentions. Catalytica recently announced the commercialization of a system which guarantees NO_x emission below 3 ppm and CO and UHC emission below 10 ppm as certified in field tests on a 1.5 MW machine.

The development of suitable catalysts has played the main role in such achievement and will be still crucial in further developments. Catalytic combustor operates under adiabatic lean conditions. Air is delivered with extremely high flow rate (>100 kg/m^2 s) from the compressor (at temperatures, which depending on the pressure ratio, can be as low as 300°C) and is premixed with natural gas at equivalent ratios up to 0.4 which correspond to adiabatic reaction temperature of 1400°C. Accordingly, the catalyst must be extremely active to guarantee low temperature ignition, and able to withstand thermal stresses associated with high operating temperatures.

The following properties make mandatory the use of palladium-based catalysts in natural gas fuelled GT combustors:

1. they have been known for a long time as the most active systems in methane combustion [1]; indeed, at short residence times of GT operations, they are the only catalysts able to provide ignition at temperatures close to that of the compressor

*Corresponding author. Tel.: +39-02-2399-3258; fax: +39-02-7063-8173; e-mail: gianpiero.groppi@polimi.it

0920-5861/99/$ – see front matter
PII: S0920-5861(98)00518-5

discharge. This minimizes the preheating with NO_x-producing diffusive burner;
2. they allow self-control of the catalyst temperature at 850–950°C during combustion of CH_4/air mixture with high adiabatic reaction temperature (1400°C), thus preventing the catalyst from too severe thermal stresses [2];
3. all the Pd species that are present under reaction conditions (metal, oxide and hydroxide) exhibit negligible volatility at T<1000°C [3].

The property of temperature self-control has been associated with the reversible $PdO \Leftrightarrow Pd^0$ transformation. Several studies have pointed out that the methane combustion activity of Pd oxide species is much more higher than that of metallic Pd [4–8]. Accordingly, temperature self-control would occur through the following mechanism: at low temperature Pd is stable in the active oxide state and effectively ignites the reaction; the increase of the catalyst temperature due to combustion light-off causes the $PdO \rightarrow Pd^0$ reduction. Due to the low methane combustion activity of metallic Pd the reaction would switch-off thus decreasing the catalyst temperature; this results in the reoxidation of Pd to PdO that in turn re-ignites the combustion. At steady state a stable temperature would be reached which is related to the characteristics of $PdO \Leftrightarrow Pd^0$ redox process and is well below the adiabatic reaction temperature.

Despite of the agreement on the general features of this mechanism many fundamental aspects deserve further investigation such as:

1. the controlling factors of palladium redox process dynamics;
2. the nature of the Pd species (bulk or skin oxide, PdO_x stoichiometry, dispersion of oxide and metal) and their associated activity and stability properties;
3. the role of metal–support interactions.

Better comprehension of such fundamental aspects could provide a significant improvement of the catalyst performances, particularly with respect to minimization of catalyst overheating associated with local runaway which is described as a major challenge in the development of commercial application with satisfactory service life (8000 h) [2]. Pilot scale experiments [9] evidenced strong excursions of the catalyst temperature, particularly during start-up, that often result in permanent damage of the catalyst.

CeO_2 is a well known promoter in noble metal-based combustion catalysts. Indeed, palladium catalysts supported on CeO_2-promoted materials have been widely investigated and are currently used in catalytic mufflers operating under alternate reducing and oxidizing environment [10]. Studies on the role of CeO_2 in this kind of applications have been recently reviewed by Trovarelli [11]. However, much less work has been done to investigate the nature of palladium–CeO_2 interactions under lean conditions.

In this work the effect of CeO_2 addition on alumina supports for Pd-based combustion catalysts operating under lean condition is addressed. For this purpose binary and ternary supports have been prepared by impregnation of La_2O_3 and/or CeO_2 onto transition alumina and characterized by means of XRD and L-Raman spectroscopy, BET surface area and TPR experiments. Over palladium catalysts obtained with these supports, the characteristics of $PdO \Leftrightarrow Pd^0$ transformation have been investigated by TG experiments with repeated heating/cooling cycles in air. Finally, activity tests in CH_4 combustion have been performed under both steady state and temperature cycled conditions. The major aim of the work has been to clarify the influence of CeO_2 on $PdO \Leftrightarrow Pd^0$ transformation and its relevance with respect to CH_4 combustion properties.

2. Experimental

2.1. Preparation

A γ-Al_2O_3 sample of 200 m^2/g obtained by calcination at 700°C for 10 h of a commercial pseudobohemite powder precursor has been used as starting material. All the samples, supports and Pd-containing catalysts have been prepared via impregnation using the incipient wetness technique.

2.1.1. Supports

For preparation of supports the impregnation has been performed using $La(NO_3)_3 \cdot 6H_2O$ (Aldrich 99.99%) and $Ce(NO_3)_3 \cdot 6H_2O$ (Aldrich 99%) as precursors.

Weighted amounts of La and Ce precursors have been deposited on the samples to obtain two binary samples containing 5% (w/w) of La_2O_3 and 11.5% (w/w) of CeO_2, respectively, and one ternary sample containing 5% (w/w) of La_2O_3 and 11.5% (w/w) of CeO_2. 5% (w/w) La_2O_3 loading has been chosen as the optimum amount for the stabilization of alumina on the basis of previous experimental results and of literature indications [12–14]. 11.5% (w/w) of CeO_2 has been selected as representative of typical loading in catalytic mufflers [10].

All the supports materials have been dried at 110°C overnight and then calcined at 1000°C with the following heating schedule: heating rate 60°C/h, hold at the final temperature 10 h, cooling rate 100°C/h.

The ternary support, i.e. La/Ce/Al, has been obtained through the following steps:

1. impregnation with the La solution;
2. overnight drying at 110°C and calcination at 1000°C for 10 h;
3. impregnation with the Ce solution;
4. overnight drying at 110°C and calcination at 1000°C for 10 h.

Such in series preparation procedure was followed according to [15].

All the systems were further calcined at 1050°C and 1100°C for 10 h for characterization purposes.

In the following the supports will be quoted as: *x*La*y*Ce-*T*(°C), e.g. the notation 5La11.5Ce-1050 identifies the 5%La_2O_3–11.5%CeO_2/Al_2O_3 ternary support calcined at 1050°C. Undoped alumina will be quoted as Al-*T*(°C).

Two additional systems have been prepared for characterization purposes: pure CeO_2 and a 11.5% (w/w) CeO_2 supported on non-porous α-Al_2O_3 (Aldrich 99.9%). Pure CeO_2 has been obtained via decomposition of $Ce(NO_3)_3{\cdot}6H_2O$ by calcination above 350°C; the α-Al_2O_3 supported CeO_2 has been prepared according to the same procedure described above.

2.1.2. Pd-containing catalysts

A $Pd(NO_3)_2$ solution (Aldrich 99.99%) containing 10% (w/w) Pd and 10% (w/w) HNO_3 has been used as Pd precursor. 2.5% and 5% (w/w) of Pd (as metal), have been deposited on the different supports calcined at 1000°C before impregnation.

Pd-containing materials have been dried at 110° overnight and then calcined at 1000°C with the following heating schedule: heating rate 60°C/h, hold at the final temperature 10 h, cooling rate 100°C/h.

In the following the Pd catalysts will be quoted as: *x*Pd*y*La*z*Ce-*T*(°C), e.g. the notation 5Pd5La11.5Ce-1000 identifies the sample containing 5% (w/w) of Pd deposited on the ternary support and calcined at 1000°C.

2.2. Characterization

The samples have been characterized by different physico-chemical techniques.

2.2.1. X-ray powder diffraction

Spectra have been collected using a Philips vertical goniometer (PW 1050/70). The Ni-filtered Cu-k_α radiation (λ=1.5418 Å) and the following experimental conditions have been used: range=10–70° 2θ, step size=0.05° 2θ, time per step=12.5 s.

Crystallite dimensions (τ) of CeO_2 and PdO have been calculated from diffraction line broadening [16], considering the (1 1 1) reflection for CeO_2 and the (1 1 2) reflection for PdO. For this purpose the spectrum of the single reflection has been collected using more accurate experimental conditions (step size=0.005° 2θ, time per step=7 s). The maximum position and the FWHM (full width at half maximum) have been evaluated by the profile fitting routine of the Philips PC-APD diffraction software.

2.2.2. Morphological analysis

Specific surface areas (S_a) of the samples have been measured by the N_2 adsorption technique (BET method) using a Fisons Sorptomatic instrument (1900 series). The catalyst pore volume has been estimated by means of water adsorption, whereas the average pore diameter has been calculated with the equation $A_s=(2V_p/r_p)$ under the hypothesis of monomodal distribution and cylindrical-shaped pores.

2.2.3. Laser-Raman spectroscopy

Laser-Raman (LR) spectra have been collected using a double monochromator Dilor XY 500 spectrometer equipped with a CCD detector (Spectrum One Jobin Yvon Spex) and an Olympus BH2 microscope. A green laser beam (514.5 nm) has been used as

exciting line under the following experimental conditions: laser power=200 mW, acquisition time=60 s, slit=200 μm, number of accumulations=10.

2.2.4. Thermal gravimetric analyses

TG diagrams have been collected in air with a simultaneous TG-DTA 6300 Seiko instrument. The following experimental parameters have been used: loaded sample weight 15–20 mg; flow rate 200 ml/min; heating and cooling rate 20°C/min. Three cycles of heating and cooling in the 450–1000°C range have been performed.

2.2.5. Temperature programmed reduction

TPR experiments were carried out in a quartz microreactor (i.d. 6 mm) loaded with 200 mg of catalyst. The microreactor was inserted in a furnace driven by a PID temperature programmer-controller. For all the experiments, 5% H_2/Ar at a flow rate of 35 Ncc/min was used as a reducing gas, and the heating rate was 10°C/min. H_2 consumption was monitored by a TCD detector after removal of water in a molecular sieve trap.

2.3. Catalytic activity tests

2.3.1. Steady state tests

Combustion tests have been performed using a quartz microreactor (i.d. 7 mm) equipped with a sliding thermocouple loaded with 110 mg of powder catalyst with small particle size (d_p=0.1 mm). Quartz powder with the same particle size has been added for dilution (w_{cat}/w_{dil}=2/1). Small particle size and dilution have been adopted in order to minimize diffusional limitations and temperature gradients in the reactor, respectively. The reactor has been operated at near atmospheric pressure (140–160 kPa due to pressure losses in the catalyst bed.) It has been fed at GHSV=210 000 Ncc/g_{ctz} h with 0.5% CH_4 and 2%, 21% and 98% of O_2 (N_2 to balance). Analysis of products and reactants has been performed by on line gas chromatography. Further details are reported elsewhere [17].

2.3.2. Transient tests

Transient flow-microreactor experiments have been performed in a quartz tubular fixed bed microreactor (i.d. 7 mm) loaded with 70 mg of catalyst ($d_p \cong 0.1$ mm) diluted with 140 mg of quartz granules. The reactor has been operated at near-atmospheric pressure (P=120–140 kPa abs. due to pressure drops in the catalyst bed) and has been inserted into an electric furnace driven by a proportional-integral-derivative temperature controller/programmer (Eurotherm 812). The temperature of the catalyst has been measured and controlled by means of a *K*-type thermocouple (o.d.=0.5 mm) sliding in a quartz thermocouple (o.d.=2 mm) well directly immersed in the catalyst bed.

The reactant gases have been fed to the reactor by means of electronic mass-flow meter-controller (Brooks 5850 TR). The various gases, coming from calibrated gas cylinders (SAPIO) were blended before entering the reactor. The overall flow rate has always been maintained at 180 Ncc/min, so that the reactor operated at GHSV=154 000 Ncc/(g_{cat} h). For the analysis of the exiting gases, the reactor outlet has been connected to a quadrupole mass detector (Balzers QMS 200).

In a typical transient methane oxidation experiment, a stream of CH_4 (5000 ppm)+O_2 (2% (v/v)) in He was fed to the reactor at room temperature. When the mass-spectrometer signals were stabilized, the catalyst temperature was linearly raised at 15°C/min up to 400°C and at 10°C/min up to 900°C. Then, the temperature was decreased at 10°C/min down to near 400°C, while continuously monitoring the concentration of the gases exiting from the reactor. Accordingly, the reactivity of the catalyst could be monitored both upon increasing and decreasing temperature.

The following mass-to-charge ratios (*m*/*e*) have been used to monitor the concentrations of products and reactants: 15 and 16 (CH_4), 18 (H_2O), 28 (CO), 32 (O_2), 44 (CO_2). The data have been quantitatively analyzed by taking into account the response factors and the overlapping of the fragmentation patterns experimentally determined.

3. Results and discussion

3.1. Characterization of supports

3.1.1. XRD and morphology

In Fig. 1 the XRD spectra of 5La-1000, 11.5Ce-1000 and 5La11.5Ce-1000 are reported, whereas

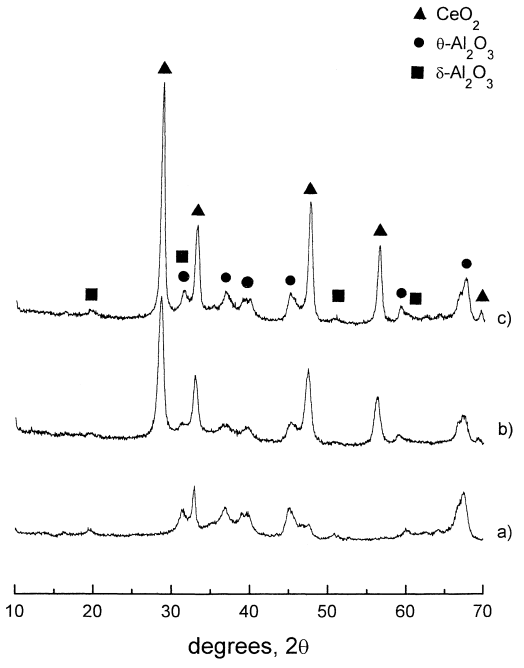

Fig. 1. XRD spectra of the different supports calcined at 1000°C: (a) 5La-1000; (b) 5La11.5Ce-1000; (c) 11.5Ce-1000.

Table 1 reports morphological data for all the supports calcined in the 1000–1100°C temperature range.

The 5La-1000 sample exhibits the reflections of transition δ- and θ-Al_2O_3 only (JCPDS 16-394 and 35-121, respectively,) along with a surface area of 124 m^2/g. No reflections of α-Al_2O_3 are detected in the XRD spectra of this system upon calcination at 1050°C and 1100°C, that result in a surface area of 89 and 72 m^2/g, respectively. Inhibition of α-Al_2O_3 formation and retention of relatively high surface area values are in line with alumina stabilization by La_2O_3 addition which is well documented in [12–14]. Such stabilization effect is favored by the high dispersion of La_2O_3 evidenced by the absence of any crystallized La-containing phase, that is in line with the tendency of La^{3+} to spread over the surface of transition alumina [18].

In the sample 11.5Ce-1000, which exhibits a surface area of 95 m^2/g, the reflections of well-crystallized CeO_2 [JCPDS 4-539] with fluorite-type structure are evident along with those of δ- and θ-Al_2O_3. Calcination at 1050°C and 1100°C results in a progressive crystallization of CeO_2, as evidenced by the narrowing of the corresponding reflections, and a decrease of surface area down to 73 and 45 m^2/g, respectively. Such sintering is accompanied by the appearance of increasing amount of α-Al_2O_3 in the XRD spectra of 11.5Ce-1050 and 11.5Ce-1100. Similar calcination treatment performed over undoped alumina samples results in higher amounts of α-Al_2O_3 and in surface areas of 69 and 21 m^2/g at 1050°C and 1100°C, respectively. Accordingly also addition of large amounts of CeO_2 inhibits sintering and phase transition of alumina in line with previous literature reports [11]. Such an effect, however, is much less pronounced than that observed for La_2O_3.

Also in the ternary 5La11.5Ce-1000 sample the reflections of crystalline CeO_2 are well evident along with the presence of the features of δ- and θ-Al_2O_3. Accurate evaluation of the position of the maximum of the reflections of CeO_2 ((1 1 1), (2 0 0), (2 2 0) and (3 1 1)) by profile fitting analysis has evidenced a coherent 2θ shift toward lower angles in the range 0.10–0.15 with respect to the position of the same peaks in 11.5Ce-1000. This is likely due to the dissolution of La^{3+} ions in the CeO_2 lattice allowed by similarity of ionic radii (La^{3+}=1.19 Å, Ce^{4+}=0.97 Å) [19]. The larger size of La^{3+} ion causes lattice expansion that in turn results in the observed 2θ shift. Also for the ternary sample calcinations at 1050°C and

Table 1
Morphological data of samples 5La, 11.5Ce and 5La11.5Ce at different calcination temperatures

Sample	T_{calc}=1000°C				T_{calc}=1050°C				T_{calc}=1100°C			
	As (m^2/g)	V_p (mm^3/g)	d_p (Å)	τ_{CeO2} (Å)	As (m^2/g)	V_p (mm^3/g)	d_p (Å)	τ_{CeO2} (Å)	As (m^2/g)	V_p (mm^3/g)	d_p (Å)	τ_{CeO2} (Å)
5La	124	950	300	–	89	900	400	–	72	800	440	–
11.5Ce	95	900	400	160	73	800	440	200	45	600	540	270
5La11.5Ce	97	900	380	110	86	800	380	130	58	800	560	180

1100°C result in a progressive crystallization of CeO_2 along with a loss of surface area that decrease down to 86 and 58 m^2/g, respectively. However similarly to the binary La-containing sample, no reflections of α-Al_2O_3 are observed, thus suggesting that the alumina stabilization of dispersed La_2O_3 is still effective in the presence of large amount of CeO_2 despite of formation of La–Ce oxide solid solution.

As mentioned above in both the binary and the ternary Ce-containing supports the presence of well-crystallized fluorite-type CeO_2 is observed. However, crystal size of CeO_2 particles appears to be lower with respect to literature indication on sintering behavior of CeO_2 [20] so that a significant effect of the support against CeO_2 sintering can be conceived. To further investigate this point two samples consisting of pure CeO_2 and 11.5% (w/w) CeO_2 supported on non-porous α-Al_2O_3 have been prepared and calcined at 1000°C, 1050°C and 1100°C for 10 h. Crystallite dimensions of CeO_2 evaluated from FWHM in the XRD spectra of the calcined samples are reported in Fig. 2 along with those evaluated for the 11.5Ce and 5La11.5Ce. In all the systems CeO_2 crystallites grow on increasing the calcination temperature. However it is apparent that supporting CeO_2 on porous transition alumina markedly affects the crystal size. In pure CeO_2 crystallites grow from 500 to 600 Å in the 1000–1100°C calcination temperature range. This is in line with literature indication [20] on CeO_2 sintering, that indicate a complete surface area loss of pure Ce oxide upon calcination above 800°C. The non-porous α-Al_2O_3 supported sample shows CeO_2 crystallite dimensions of 350 Å upon calcination at 1000°C. Such dimensions are quite larger than the values reported in Table 1 calculated for the transition alumina supported samples (100–150 Å). CeO_2 crystallites on non-porous α-Al_2O_3 further grow on increasing the calcination temperature up to 600 Å at 1100°C, i.e. the same value calculated for pure CeO_2. On the other hand on 11.5Ce-1100 and 5La11.5Ce-1100, CeO_2 crystal size is limited at 250 and 180 Å, respectively. Comparison between the transition alumina supported samples also shows that addition of La_2O_3 on the alumina surface before the impregnation with CeO_2 results in lower dimension of CeO_2 crystallites. Enhancement of CeO_2 dispersion, as determined by XPS measurements, on a La-doped γ-Al_2O_3 support prepared via a similar procedure to that adopted herein have been reported by Graham et al. [15].

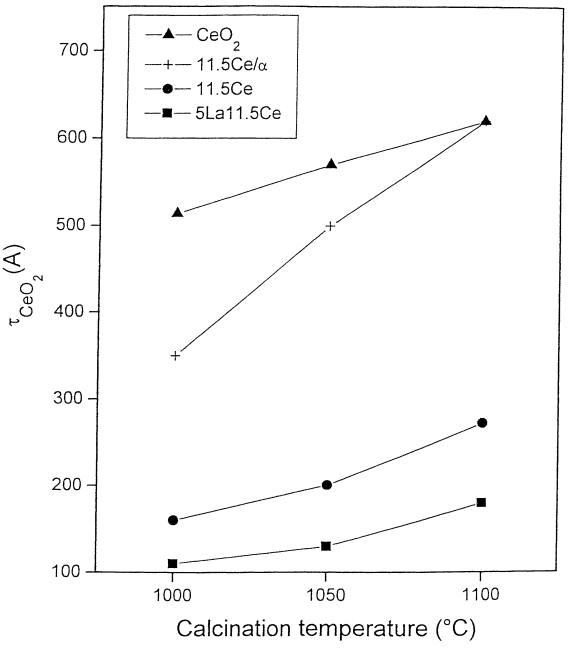

Fig. 2. Crystallite dimensions of CeO_2 at different calcination temperatures. (▲) pure CeO_2; +11.5CeO_2/α-Al_2O_3; (●) 11.5Ce; (■) 5La11.5Ce.

Comparison of the crystallite dimensions of CeO_2 on porous transition alumina reported in Fig. 2 with the pore diameters evaluated from water adsorption (see Table 1) shows that the crystal size is always lower, although comparable, than pore diameter. Accordingly it can be argued that the control of CeO_2 sintering is governed by the porosity of the support, i.e. CeO_2 crystallites grow within the pores so that their dimension cannot exceed the pore diameter.

According to this mechanism, the promoting effect of La_2O_3 on CeO_2 dispersion can be associated with the inhibiting effect of La_2O_3 on Al_2O_3 sintering, although pore size data in Table 1 do not provide clear indication on this effect. Besides, incorporation of La^{3+} in the CeO_2 lattice has been reported in the literature to lower the sintering rate at 730°C [21].

It is worth noticing that due to the large porosity of transition aluminas (typically 0.8–0.9 cm^3/g) this sintering control mechanism can be effective at high CeO_2 loadings.

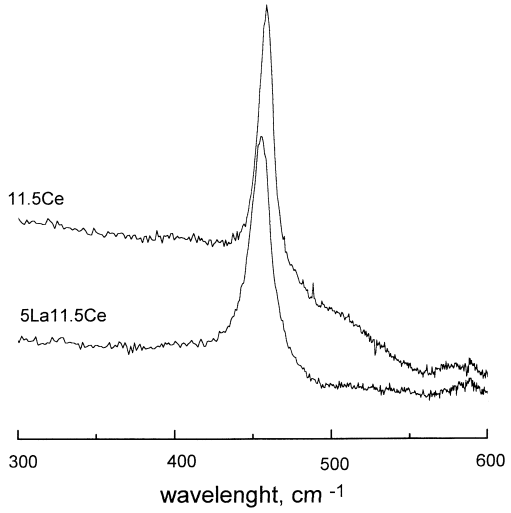

Fig. 3. Laser-Raman spectra of 5La11.5Ce-1000 and 11.5Ce-1000.

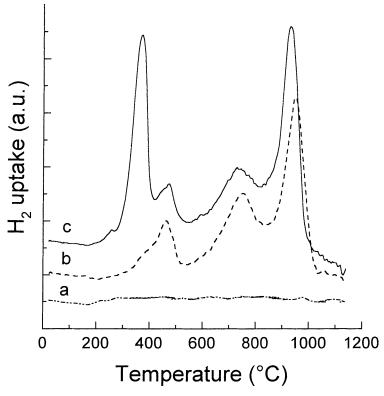

Fig. 4. Results of TPR experiments performed over 5La-1000 (a), 11.5Ce-1000 (b) and 5La11.5Ce-1000 (c).

3.1.2. L-Raman spectroscopy

In Fig. 3 the L-Raman spectra of 11.5Ce-1000 and 5La11.5Ce-1000 collected in the 300–600 cm^{-1} range are reported. In both the spectra the following features are observed that according to literature indication [22] have been interpreted as follows:

1. a strong narrow peak at 460 cm^{-1} which is associated with F_{2g} Raman active mode characteristic of crystalline CeO_2 with fluorite-type structure;
2. a weak band at 590 cm^{-1} attributed to distortion of the fluorite-type structure;
3. a fluorescence band in the range 300–550 cm^{-1} associated with small amounts of $CeAlO_3$.

Noticeably, the broadening of the band at 460 cm^{-1} in the ternary La-containing sample, confirms the smaller crystallite dimension of CeO_2 in this sample [23]. From FWHM of the L-Raman bands at 460 cm^{-1} crystallites dimension of 100 and 200 Å for 11.5Ce-1000 and 5La11.5Ce-1000, respectively, have been calculated. These data, along with those obtained by XRD measurements (Table 1), are in line with the smaller sintering of CeO_2 in presence of La_2O_3.

3.1.3. TPR experiments

The results of the TPR experiments performed over 5La-1000, 11.5Ce-1000 and 5La11.5Ce-1000 are shown in Fig. 4 (curves (a)–(c), respectively), where the various traces have been shifted vertically for clarity. The TPR profile shows that the 5La-1000 sample (curve (a)) is not reduced by H_2 up to 1100°C. A different behavior is apparent for the 11.5Ce-1000 sample (curve (b)): indeed in this case three reduction peaks are visible in the TPR profile, with maxima near 450°C, 720°C and 900°C. In line with literature reports [22,11], these peaks can be associated with the reduction of the surface oxygen of CeO_2 (peak at 450°C), with the formation of $CeAlO_3$ (peak at 720°C) and with the reduction of CeO_2 to Ce_2O_3 (peak at 900°C).

In the case of the 5La11.5Ce-1000 support (curve (c)), in addition to the TPR peaks already observed near 450°C, 720°C and 900°C for the 11.5Ce-1000 sample (curve (b)), a new reduction peak is evident at low temperatures, near 370°C. The overall amount of H_2 consumed in this case indicated that a complete reduction of Ce^{4+} to Ce^{3+} has been achieved for 5La11.5Ce-1000, whereas in the case of the 11.5Ce-1000 sample the degree of reduction is lower, near 80%. This suggests that the addition of La to 11.5Ce-1000 increases the reducibility of CeO_2. It is speculated that the non-reducible Ce^{4+} species present in the 11.5Ce-1000 sample and roughly accounting for 20% of total Ce can be reduced in the 5La11.5Ce-1000 sample possibly due to a specific interaction with the La component. As a matter of facts, evidence have been collected from the XRD data previously shown for the formation of La–Ce solid solutions in

5La11.5Ce-1000 in which La^{3+} ions are dissolved into the CeO_2 lattice. The dissolution of La^{3+} ions results in the formation of oxygen vacancies in the Ce lattice because of charge neutralization. Therefore, it is likely that this enhances the availability of lattice oxygen of the sample. Similar effects have been reported by Miki et al. [24], even if in this case the oxygen storage capacity of the samples has been observed to increase only in the presence of precious metals that activate the H_2 molecule thus accelerating the reaction with lattice oxygen.

3.2. Characterization of Pd supported catalysts

3.2.1. XRD and morphology

In the XRD spectra of 2.5Pd5La-1000, 2.5Pd11.5Ce-1000 and 2.5Pd5La11.5Ce-1000 the same phases already described for the corresponding supports are observed except for the presence of crystalline PdO [JCPDS 6-515]. The reflections of this phase have also been detected in the XRD spectrum of undoped 2.5PdAl-1000 along with those of δ-θ- and α-Al_2O_3. Calculated crystallite dimensions of PdO are reported in Table 2. In all the investigated samples similar values of the crystal size of PdO have been obtained, ranging from 120 to 190 Å. These values closely resemble those of CeO_2 (160 and 120 Å for 11.5Ce-1000 and 5La11.5Ce-1000, respectively), thus suggesting that the sintering mechanism of PdO is similar to that described above for CeO_2 and it is governed by the porosity of the support.

3.2.2. Thermogravimetric analysis

The $PdO \Leftrightarrow Pd^0$ dynamic redox behavior has been investigated by means of TG measurements with repeated heating and cooling cycles. To clarify the role of the support on the $PdO \Leftrightarrow Pd^0$ transformation in addition to binary 11.5Ce-1000 and 5La-1000 systems and to ternary 5La11.5Ce-1000, also an undoped alumina sample calcined at 1000°C (Al-1000) has been used as support material. All the systems have been loaded with 5% (w/w) Pd in order to magnify weight variations associated with temperature cycles. XRD spectra of 5PdAl-1000, 5Pd5La-1000, 5Pd11.5Ce-1000 and 5Pd5La11.5Ce-1000 have evidenced the same phase composition of the corresponding 2.5% (w/w) Pd-loaded catalysts. Also, the calculated crystal size of PdO that are reported in Table 2, compare well with those calculated in the case of the samples with 2.5% (w/w) of Pd. This indicates that in the investigated range, Pd loading has not a significant effect on PdO dispersion. Finally, it is worth noticing that TG experiments performed on samples with 2.5% (w/w) of Pd have shown similar features of $PdO \Leftrightarrow Pd^0$ transformation.

In Fig. 5 the thermograms collected in air over all the investigated samples during three subsequent heating and cooling cycles between 450°C and 1000°C are

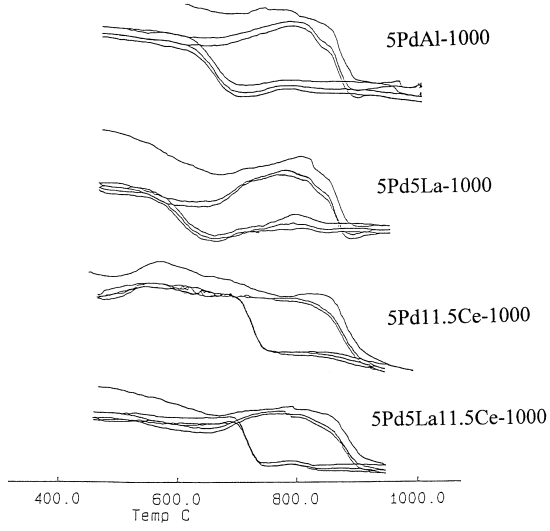

Fig. 5. Results of TG experiments over the different Pd catalysts calcined at 1000°C.

Table 2
Crytallite dimensions of PdO on different supports calcined at 1000°C

Pd% (w/w)	τ_{PdO} (Å) on different supports			
	Al-1000	5La-1000	11.5Ce-1000	5La11.5Ce-1000
2.5	150	120	170	190
5	140	100	170	150

reported. All the samples show a similar behavior. During the heating ramp, starting from 800–860°C depending on the support, a progressive weight loss is observed, that proceeds to constant weight which is reached about 100°C above. The overall weight loss corresponds well to the theoretical value associated with the $PdO \rightarrow Pd^0$ decomposition. During the cooling ramp, the weight remains constant down to a temperature that is always markedly lower than that observed for the onset of weight decrease in the heating ramp and that depends on the support material. Below this temperature a weight increase is observed which is equivalent to the weight loss in the heating ramp, thus originating a typical hysteresis. Such behavior is reproduced in repeated cycles and resembles well literature statement for $PdO \Leftrightarrow Pd^0$ reversible transformation in Pd-based systems [4].

To better evidence the effect of the support on the characteristics of the $PdO \Leftrightarrow Pd^0$ redox process, the initial and the final temperature of the $PdO \rightarrow Pd^0$ reduction (IRT and FRT), as well as the initial and the final temperature of the $Pd^0 \rightarrow PdO$ oxidation (IOT and FOT) are summarized in Table 3 along with the corresponding weight variations. It is apparent that the nature of the support affects both reduction and reoxidation phenomena. With respect to the $PdO \rightarrow Pd^0$ reduction 5Pd5La-1000 behaves similarly to Pd supported on undoped alumina. On both these samples PdO decomposition starts at about 800°C, is completed at 880°C and apparently proceeds through at least two steps, as evidenced by the marked change of the slope of the TG curve at 830–840°C. In the 5Pd11.5Ce-1000 sample the reduction of PdO starts at 860°C, i.e. 60°C above than in samples without ceria, and it is completed at 920°C. In this case no appreciable changes in the slope of weight decrease are observed and apparently reduction proceeds through a single step. On the ternary support in which both CeO_2 and La_2O_3 are present, PdO decomposition occurs in the same temperature range and proceeds very similarly to 5Pd11.5Ce-1000.

The effect of the support on $Pd^0 \rightarrow PdO$ reoxidation is more pronounced. In 5Pd5La-1000 formation of PdO starts about 50°C below than on the undoped alumina supported sample. Conversely, CeO_2 promotes Pd^0 reoxidation that in 5Pd11.5Ce-1000 starts at 740°C, i.e. 60°C above with respect to 5PdAl-1000 and is completed at 690°C.

Despite of the retarding effect on Pd^0 reoxidation observed on 5Pd5La-1000, the ternary support obtained by consecutive impregnation of La_2O_3 and CeO_2 onto the alumina surface has a similar behavior to the binary CeO_2-promoted alumina, with Pd^0 reoxidation occurring in the same temperature range.

The effect of alumina promoters on $PdO \Leftrightarrow Pd^0$ redox process can be summarized as follows:

1. La_2O_3 does not affect PdO decomposition and hinders Pd^0 reoxidation;
2. CeO_2 stabilizes PdO, since it hinders PdO reduction and promotes Pd^0 reoxidation: indeed both these processes occur at temperatures 50–60°C higher than on the undoped support;
3. when La_2O_3 and CeO_2 are added in consecutive steps, the effect of the latter dominates and the ternary system behaves very similarly to the binary CeO_2 promoted one.

Similar support effects have been already reported in the technical literature. Kennely and Farrauto [25] investigated the effect of the addition of lanthanide promoters onto the alumina surface by means of TG experiments similar to those described in this work. With La loadings up to 6% (w/w), comparable to that adopted in this work, these authors found an inhibiting

Table 3
Initial and final reduction and oxidation temperatures from TG experiments over Pd catalysts supported on different materials

Sample	Reduction		Oxidation		ΔWeight (%)
	IRT (°C)	FRT (°C)	IOT (°C)	FOT (°C)	(Expected=0.7%)
5PdAl-1000	800	890	675	600	0.6
5Pd5La-1000	800	880	630	540	0.6
5Pd11.5Ce-1000	860	920	740	690	0.7
5Pd5La11.5Ce-1000	850	920	740	690	0.6

effect on Pd^0 reoxidation similar to that herein described. On the other hand for higher La loading (11.5% (w/w)) they report an opposite marked promoting effect of La on Pd^0 reoxidation. However, they do not provide any explanation for this complex behavior.

Kennely and Farrauto [25] also disclosed in a patent that CeO_2 stabilizes active PdO. Such stabilization was claimed to avoid catalyst deactivation by increasing the temperature of PdO decomposition, but also to favor catalyst regeneration by increasing the temperature of Pd^0 reoxidation. CeO_2 promotion of Pd^0 reoxidation was also reported by Shyu et al. [26]. These authors observed that on a CeO_2-doped alumina support upon reduction in H_2 at 920°C Pd^0 readily reoxidizes in ambient air. This oxidation was not observed for Pd supported on undoped alumina. They associated this behavior with the formation of intermediate Pd oxide species on the surface of partially reduced cerium oxide particles.

Both oxidation of metal palladium particles and reduction of palladium oxide have been investigated in the literature. For a SiO_2 supported palladium catalysts, Voogt [27] proposed that oxidation occurs via a shell–core mechanism with lattice reconstruction needed for the formation of a new oxide layer at the oxide–metal interface as the rate controlling step. This results in a strongly activated process with an activation energy of at least 100 kJ/mol. Accordingly, oxidation rate is very slow at 300°C, whereas at 400°C the oxidation of metal palladium particles of 50–80 Å is almost completed after 10 min.

For a 10%Pd/ZrO_2 with Pd particle diameters of 280 Å, Su et al. [8] proposed a different two stage oxidation mechanism: first the reaction occurs via an electric field driven oxidation according to the Cabrera–Mott theory; then, when a sufficiently thick palladium oxide layer has formed, oxidation rate becomes limited by oxygen diffusion through the oxide lattice. They reported an activation energy of 100 kJ/mol for the first stage that at 500°C in 5% of O_2 is very fast and results in the oxidation of 70% of initial Pd in less than 1 min. Under the same condition 30 min are required for complete oxidation due to the onset of diffusional limitations.

Concerning PdO reduction Voogt [27] proposed that it proceeds through the formation of a metallic core that progressively grows up to a monolayer of PdO. The reduction of this skin oxide is more difficult: reduction of 130 Å PdO particles takes 60 min under vacuum condition at 500°C. By performing reduction experiments under CH_4 and H_2-containing atmosphere, Su et al. [8] evidenced that reduction mechanism markedly depends on the reducing agents. However complete reduction is achieved after about 5 min in 3% CH_4 at 260°C.

During TG experiments with heating and cooling cycles herein discussed in the presence of O_2 both PdO reduction and Pd^0 oxidation occurs under quite different conditions from those used in the studies described above: during heating ramps the presence of oxygen stabilizes PdO up to temperature ranging from 800°C to 860°C depending on the support material. These temperatures are representatives of actual conditions in adiabatic combustors. In cooling ramps reoxidation occurs at lower temperature but still much higher than those in the studies above, particularly with CeO_2-containing supports.

In line with the literature indication reported above at such temperature the rates of reduction and oxidation are expected to be very fast, so that it is expected that they negligibly affect the shape of TG cycles obtained with the heating rates of 20°C/min. To investigate this point a TG experiment has been performed on the 5PdAl-1000 sample with a heating and cooling rate of 10°C/min. The results are compared in Fig. 6 with those obtained over the same sample with temperature ramps of 20°C/min. The two thermograms are almost perfectly overlapped so that it can be assumed that PdO⇔Pd^0 reversible transition is not controlled by kinetics at such heating rates. Similar results were obtained by Dalla Betta et al. [28] that

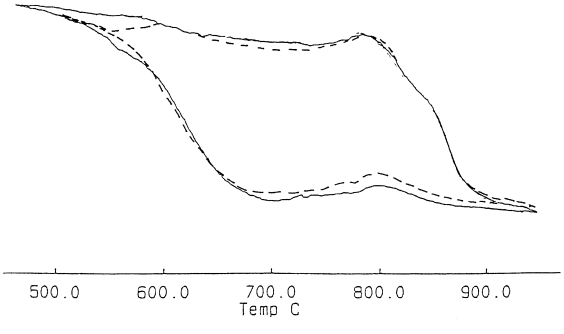

Fig. 6. TG cycles of 5PdAl-1000 performed at different heating–cooling rates: full line 20°C/min; dotted line 10°C/min.

using a palladium oxide powder observed that on decreasing the heating rate from 10 to 5°C/min, the temperature observed for $PdO \rightarrow Pd^0$ transition in air (795°C) did not change.

These results suggest that the $PdO \Leftrightarrow Pd^0$ transition is governed by thermodynamic factors and not by kinetics under the conditions of TG experiments in this work. Accordingly also the PdO stabilization effect of CeO_2 observed in our TG experiments is likely related to thermodynamic factors and not to the kinetics of the redox process. Work is in progress to better clarify these aspects.

Still the mechanism through which CeO_2 affects the thermodynamic state of PdO and/or Pd^0 has not been clarified and deserves further investigation.

3.3. Catalytic activity tests

3.3.1. Steady-state catalytic activity tests

In Fig. 7(a) and (b) conversion curves obtained in steady-state CH_4 combustion experiments performed with different O_2 concentration over 2.5Pd5La-1000 and 2.5Pd5La11.5Ce-1000 are reported, respectively. On both the samples very small variation of conversion at fixed temperatures occurs on changing the O_2 concentration by a factor 50. It has to be reminded that the lowest O_2 feed concentration herein investigated (2%) is twice the stoichiometric amount required to complete CH_4 combustion. These data evidence that P_{O_2} does not significantly affects low temperature activity in CH_4 combustion of the investigated Pd-based catalysts when large O_2 excess is present.

Comparison of conversion curves in Fig. 7(a) and (b) evidences that 2.5Pd5La-1000 and 2.5Pd5La11.5Ce-1000 exhibit very similar activity, thus it is apparent that the addition of CeO_2 on La_2O_3-stabilized alumina does not significantly affects the light-off performances of the corresponding Pd-based catalyst.

3.3.2. Transient catalytic activity tests

Fig. 8 shows the conversion of methane as a function of temperature measured under transient conditions in the presence of the 2.5Pd5La-1000 catalyst (dotted lines) and the 2.5Pd5La11.5Ce-1000 sample (solid lines).

In the case of the 2.5Pd5La-1000 catalyst, Fig. 8 shows that CH_4 ignites near 260°C and complete conversion is reached near 450°C, in nice agreement with the steady-state data shown in Fig. 7(a). Above 450°C the methane conversion remains complete up to the maximum investigated temperature, i.e. 900°C. A different behavior is however observed when the reaction temperature is decreased with the same heating schedule from 900°C to 400°C: indeed in this case a decrease in the methane conversion is observed

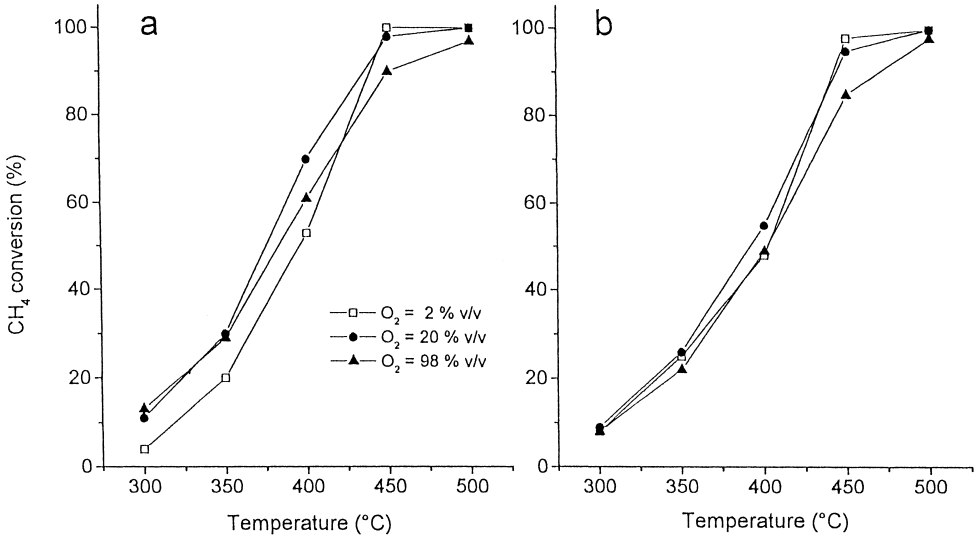

Fig. 7. Results of steady-state CH_4 oxidation experiments performed over 2.5Pd5La-1000 (a) and 2.5Pd5La11.5Ce-1000 (b).

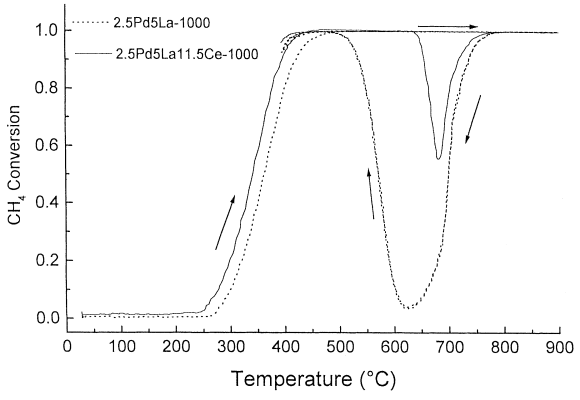

Fig. 8. Results of transient CH_4 oxidation experiments performed over 2.5Pd5La-1000 (dotted lines) and 2.5Pd5La11.5Ce-1000 (solid lines). Heating rate: 15°C/min from RT to 400°C; 10°C/min from 400°C to 900°C; 10°C/min from 900°C to 400°C.

below 770°C, and values close to only 5% are measured at 620°C. Below this temperature the methane conversion increases on decreasing the reaction temperature and complete conversion is reached again at 450°C, where the methane conversion equals that measured on the fresh catalyst during the first heating up.

The data presented above points out the existence of an hysteresis cycle, typical of Pd supported catalysts, for which evidences have been already provided in [25]. In line with TG data reported above, the hysteresis behavior of the catalysts is associated with the occurrence of the $PdO \Leftrightarrow Pd^0$ transformation. As a matter of facts, TG analysis performed over the same catalyst sample clearly indicated that PdO is reduced to Pd^0 above 800°C, whereas metallic Pd is reoxidized by gas-phase oxygen below 680°C. Accordingly, the hysteresis observed in Fig. 8 can be easily rationalized by considering that during the heating up of the catalyst from RT (i.e. in the upper branch of the hysteresis loop), palladium is present as PdO, a species that is well known to be very active in combustion reactions [4–8,30]. Above 800°C, as suggested by TG data, PdO is reduced to Pd^0, which is much less reactive than PdO [4–8,29]. However, in spite of the suggested $PdO \rightarrow Pd^0$ transformation, no effects are visible in the CH_4 conversion vs. temperature plot, because in this high temperature region the less reactive Pd^0 species can still guarantee complete methane conversion. Also, as will be reported elsewhere [30], the pure supports are well active in this region, and the contribution of homogeneous gas-phase reactions cannot be excluded as well.

On the other hand, when the catalyst temperature is decreased from 900°C down to 400°C, the methane conversion follows the lower branch of the hysteresis loop since palladium is now present as Pd^0 that being less active than PdO, does not sustain complete CH_4 conversion below 800°C. However, below 630°C the methane conversion increases on decreasing the reaction temperature due to the reoxidation of Pd^0 to the more reactive PdO, as suggested by TG data. This process is seen at lower temperatures if compared to the TG measurements performed in air (620°C vs. 680°C): in line with the influence of the thermodynamic factors previously invoked on the $Pd^0 \rightarrow PdO$ transformation, the observed temperature shifts can be ascribed to the different O_2 partial pressure used in TG and transient reactivity experiments (20% vs. 2% (v/v)).

Therefore, the observed hysteresis loop originates from the fact that:

1. the reactivity of PdO is higher than that of Pd^0;
2. the temperature threshold for the onset of the $PdO \rightarrow Pd^0$ transformation differs from that of the reverse $Pd^0 \rightarrow PdO$.

An interesting feature of the repeated heating–cooling cycles shown in Fig. 8 is that below 500°C the reactivity of the catalyst is apparently slightly higher with respect to the first catalyst heating up. Successive heating–cooling cycles overlap these new values of the methane conversion, indicating that the activity of the catalyst has now been stabilized. The increase in the activity of a Pd/ZrO_2 sample upon cycling the catalyst has also been reported by Carstens et al. [30], and has been related to the formation of a stable state in which PdO is formed reproducibly. Similar effects have also been observed in the course of our steady-state experiments, and further studies are now in progress in order to clarify these aspects.

The behavior of the Ce-doped catalyst (2.5Pd5La11.5Ce-1000) in the catalytic combustion of methane has also been investigated. The results (solid lines of Fig. 8) show that the reactivity of this catalyst differs from that of the unpromoted sample since the hysteresis loop is still present but is less

evident. Indeed the activity drop that is observed upon decreasing the reaction temperature is markedly lower if compared to that of the Ce-free catalyst, the methane conversion reaching a minimum of 55% near 680°C. In line with the reasons discussed above concerning the origin of the hysteresis loop, the observed differences can be associated to the easier reoxidation of Pd^0 to PdO that accordingly occurs in the 2.5Pd5La11.5Ce-1000 catalyst 60°C above the 2.5Pd5La-1000 sample. This datum is in good agreement with the TG results previously shown and further provides another piece of evidence on the stabilization of the active PdO phase in the presence of CeO_2.

4. Conclusions

The effects of CeO_2 and La_2O_3 addition to alumina-supported palladium catalysts have been investigated through different characterization techniques and CH_4 combustion tests.

Characterization of the supports has evidenced that La_2O_3 is spread onto the alumina surface inhibiting its transition and sintering, whereas CeO_2 aggregates in crystals whose dimensions are controlled by the support porosity. A similar mechanism is likely responsible for the control of PdO particle dimensions.

In ternary La_2O_3–CeO_2-promoted alumina the formation of a La–Ce oxide solid solution has been detected which is likely responsible for the enhancement of CeO_2 reducibility.

TG analyses on palladium catalysts confirm the occurrence of reversible $PdO \Leftrightarrow Pd^0$ transformation in the presence of O_2 which originates a characteristic hysteresis due to different reduction and oxidation temperatures.

Such temperatures markedly depend on the nature of the support. In particular in the presence of ceria temperatures of reduction of PdO and reoxidation of Pd^0 are both shifted 50–60°C above with respect to the corresponding temperature observed on CeO_2-free samples.

Activity tests in CH_4 combustion under lean conditions show that addition of ceria on La_2O_3-stabilized alumina does not significantly affect light-off performances, but markedly affects high temperature catalytic behavior in line with its effect of stabilization of active PdO species.

Acknowledgements

Financial support for this work has been provided by Consiglio Nazionale delle Ricerche (CNR) – Roma (Italy). The author wish to thank prof. A. Trovarelli of Università di Udine for performing TPR experiments and providing assistance in their interpretation.

References

[1] R.B. Anderson, K.C. Stein, J.J. Feenan, L.J. Hofer, Ind. Eng. Chem. 53 (1961) 809.
[2] R.A. Dalla Betta, N. Ezawa, K. Tsurumi, J.C. Schlatter, S.G. Nickolas, US Patent 5 183 401, 2 February 1993.
[3] J.G. McCarty, Proceedings of EUROPACAT III, Krakow (Poland) 1997, p. 90.
[4] R.J. Farrauto, M.C. Hobson, T. Kennelly, E. Waterman, Appl. Catal. A 81 (1992) 227.
[5] F.H. Ribeiro, M. Chow, R.A. Dalla Betta, J. Catal. 146 (1994) 537.
[6] R. Burch, F.J. Urbano, Appl. Catal. A 124 (1995) 121.
[7] J.G. Mc Carty, Catal. Today 26 (1995) 283.
[8] S.C. Su, J.N. Carstens, A.T. Bell, J. Catal. 176 (1998) 125.
[9] T. Griffin, W. Weisenstein, V. Scherer, M. Fowles, Combustion and Flame 101 (1995) 81.
[10] R.M. Heck, R.J. Farrauto, in: Catalytic Air Pollution Control Commercial Technology, Van Nostrand Reinhold, New York, 1995.
[11] A. Trovarelli, Catal. Rev.-Sci. Eng. 38 (1996) 439.
[12] P. Burtin, J.P. Brunelle, M. Pijolat, M. Soustelle, Appl. Catal. 34 (1987) 225.
[13] H. Schraper, E.B.M. Doesburg, L.L. Van Reijen, Appl. Catal. 7 (1983) 211.
[14] M.F.L. Johnson, J. Catal. 123 (1990) 245.
[15] G.W. Graham, P.J. Schmitz, R.K. Usmen, R.W. McCabe, Catal. Lett. 17 (1993) 175.
[16] H.P. Klug, L.E. Alexander, in: X-ray Diffraction Procedures, Wiley, New York, 1974.
[17] G. Groppi, C. Cristiani, M. Bellotto, P. Forzatti, P.L. Villa, Appl. Catal. A 104 (1993) 101.
[18] Y.C. Xie, Y.Q. Tang, in: Advances in Catalysis, vol. 37, Chapter 1, 1990.
[19] R.D. Shannon, C.T. Prewitt, Acta Crystallogr. B 25 (1969) 925.
[20] V. Perrichon, A. Laachir, S. Abouarnadasse, O. Touret, G. Blanchard, Appl. Catal. A 129 (1995) 69.
[21] M. Pijolat, M. Prin, M. Soustelle, O. Touret, P. Nortier, Solid State Ionics 63 65 (1993) 781.
[22] J.Z. Shyu, W.H. Weber, H.S. Gandhi, J. Phys. Chem. 92 (1988) 4964.
[23] G.W. Graham, W.H. Weber, C.R. Peters, R. Usmen, J. Catal. 130 (1991) 310.

[24] T. Miki, T. Ogawa, M. Haneda, N. Kakuta, A. Weno, S. Tateishi, S. Matsuura, M. Sato, J. Phys. Chem. 94 (1990) 6464.
[25] T. Kennely, R.J Farrauto, US patent 5 216 875, 8 June 1993.
[26] J.Z. Shyu, K. Otto, W.L.H. Watkins, G.W. Graham, R.K. Belitz, H.S. Ghandi, J. Catal. 114 (1988) 23.
[27] E.H. Voogt, Palladium Model Catalysts, Ph.D. Dissertation, University of Utrecht, 1997.
[28] R.A. Dalla Betta, T. Shoji, K. Tsurumi, N. Ezawa, US Patent no. 5 326 253, 5 July 1994.
[29] J.N. Carstens, S.C. Su, A.T. Bell, J. Catal. 176 (1998) 136.
[30] Unpublished results from this laboratory..